Food Chemistry: X 32 (2025) 103229

Contents lists available at ScienceDirect

Food Chemistry: X

journal homepage: www.sciencedirect.com/journal/food-chemistry-x

Impact of drying techniques on the physicochemical, structural, thermal, techno-functional, rheological properties, and in vitro digestibility of sesame protein isolate

Osman Gul [a], Abdullah Akgün [b], Safa Karaman [c], Mahmut Ekrem Parlak [d], Furkan Turker Sarıcaoğlu [d], Senay Simsek [e,*]

[a] Department of Food Engineering, Faculty of Engineering and Architecture, Kastamonu University, Kastamonu, Turkey
[b] Department of Food Engineering, Faculty of Engineering, Trakya University, Edirne, Turkey
[c] Department of Food Engineering, Faculty of Engineering, Niğde Ömer Halisdemir University, Niğde, Turkey
[d] Department of Food Engineering, Faculty of Engineering and Natural Sciences, Bursa Technical University, Bursa, Turkey
[e] Whistler Center for Carbohydrate Research, Department of Food Science, Purdue University, West Lafayette, IN 47907, USA

ARTICLE INFO

Keywords:
Sesame protein
Drying techniques
Physicochemical property
Structure-function property
Protein functionality
Digestibility

ABSTRACT

Sesame protein isolate (SPI) is emerging as a valuable plant-based protein with promising nutritional and functional properties. This study examined the influence of three drying techniques—hot air drying (OD), spray drying (SD), and freeze-drying (FD)—on the physicochemical, structural, thermal, techno-functional, rheological properties, and in vitro digestibility of SPI. While proximate composition remained unchanged, notable variations were observed in particle size, zeta potential, FTIR spectra, free sulfhydryl (–SH) groups, and surface hydrophobicity (H_0), reflecting conformational modifications. OD-PI exhibited the highest denaturation temperature (81.83 °C) and lowest enthalpy (28.86 J/g). SD-PI demonstrated superior functional traits, including emulsion capacity (29.91 %), stability (64.83 min), foaming capacity (127.78 %), stability (47.78 %), water-holding capacity (1.81 %), and rheology, attributed to its small particle size (4.51 μm) and high solubility (72.62 %). FD-PI showed the greatest –SH and H_0 values. Importantly, SD-PI displayed enhanced digestibility, establishing spray drying as the most effective method for producing high-quality SPI for food applications.

1. Introduction

Plant-based proteins derived from oilseeds and legumes offer valuable alternatives to animal proteins. Among these, seed proteins stand out for their nutritional and functional benefits. With the growing global demand for plant-based proteins for both food and feed applications, seed proteins are increasingly being considered for their nutritional value, functional properties, and sustainability advantages. During processing, oil and other non-protein components are extracted from seeds, leaving behind a protein-rich fraction that can be utilized in a variety of formulations, including meat analogs, protein bars, and beverages. Common sources of seed proteins include soybeans, peas, sunflower, canola, and sesame, all of which offer diverse amino acid profiles suitable for various populations (Zhang, Wang, Cai, Zhao, & Zhao, 2023).

Sesame (*Sesamum indicum* L.), one of the oldest and most widely cultivated oilseed crops, is particularly rich in essential oils, proteins, and minerals. Its protein content ranges from approximately 18 % to 25 %, depending on cultivar and growing conditions (Nouska et al., 2024). In regions where animal-derived protein is scarce, sesame serves as an important dietary protein source. It contains high levels of essential amino acids, such as methionine, which is relatively limited in other plant-based proteins (Wei et al., 2022). Sesame is a versatile crop used in both human and animal nutrition and serves as the basis for a variety of processed foods such as tahini, sesame oil, and snacks (Hahm & Kuei, 2015).

Drying is a critical step in the production of seed protein concentrates, as it significantly influences both the functional properties and overall quality of the final product. Techniques such as hot air drying drying (OD), freeze drying (FD), and spray drying (SD) are commonly used to reduce moisture content of protein, thereby improving shelf life and preventing microbial growth. However, the drying conditions

* Corresponding author.
E-mail address: ssimsek@purdue.edu (S. Simsek).

https://doi.org/10.1016/j.fochx.2025.103229
Received 13 May 2025; Received in revised form 29 September 2025; Accepted 29 October 2025
Available online 31 October 2025

(temperature, pressure, and time) used in these techniques are entirely different and could significantly affect the molecular makeup and functional characteristics of proteins (Ye et al., 2024). OD is considered a simple and popular technique, which is comparatively less expensive, and drying temperature could be set below protein denaturation temperature; however, the residence time is significantly longer (Feyzi, Varidi, Zare, & Varidi, 2018). SD is the most often used drying technology for producing protein powder because it provides a high-throughput, continuous process and manipulates particle characteristics to produce an acceptable powder (Lin, Liu, Liu, & Qi, 2020). Since FD utilizes the ice sublimation mechanism at low pressure and temperature, it can preserve protein quality by ensuring no protein degradation during drying compared to SD; however, it requires significant energy and time (Lin et al., 2020; Shen, Tang, & Li, 2021).

Beyond preservation, drying also impacts key protein attributes such as texture, solubility, and bioavailability—all essential for functional and sensory performance. Proteins are inherently sensitive to heat, and thermal processing can alter functional properties like solubility, emulsification, and gelation. Heat-induced unfolding of the protein structure leads to denaturation, resulting in the loss of its natural functional properties. High temperatures can also disrupt the molecular structure of sesame seed proteins, decreasing solubility and the bioavailability of essential amino acids (Embaby, 2010). Moreover, excessive heating during drying can cause oxidation of proteins and lipids, ultimately reducing the nutritional quality of sesame seeds (Nouska et al., 2024).

There is a growing interest in developing innovative and optimized drying techniques that balance protein stability with overall product quality. Understanding the relationship between seed protein composition and drying parameters is crucial for improving the functionality and value of seed protein concentrates. Therefore, it is essential to investigate how various drying methods affect the protein content and quality of sesame seeds. Therefore, the primary objective of this study was to investigate the effects of commonly used drying techniques, including hot air drying (OD), spray drying (SD), and freeze-drying (FD)—on the physicochemical, techno-functional, and rheological properties, dynamic mechanical behavior, molecular and structural characteristics, as well as in vitro digestibility of sesame seed protein isolates.

2. Materials and methods

2.1. Materials

White sesame seeds were purchased from a local wholesaler (Aslan Sesame and Tahin Food Ltd. Co., Eskişehir, Türkiye). Before protein extraction, sesame seed oil was removed using a cold-press extraction method with a mechanical press machine (Koçmaksan KMS10, İzmir, Türkiye). The pressing temperature was fixed at 50 °C throughout the oil extraction process from the seeds. All chemicals used in this study were of analytical grade.

2.2. Extraction of protein from sesame cake

The sesame protein isolate preparation process was based on the method by Baskinci and Gul (2023). The sesame cake (95.08 % total solids, 38.07 % protein) obtained after cold-pressed oil processing was ground using a laboratory-type blender (Waring 80011S model, USA) and sieved through a 60-mesh sieve to achieve a homogeneous distribution of sesame cake powder. Afterward, sesame cake powder was mixed with distilled water at a ratio of 1:9 (*w/v*) and then the suspension was homogenized using Ultra-Turrax (Daihan, HG-15D, Gang-Won-Do, South Korea) at 9000 rpm for 3 min. After adjusting the pH of the suspension to 10.0 with 1 M NaOH, the suspension was stirred using a magnetic stirrer at 400 rpm for 1 h in order for the proteins in the cake to pass into the water. Then, the suspension was centrifuged at 8000 rpm at 4 °C for 10 min using a centrifuge (Nuve NF-800R, Türkiye) to separate the soluble proteins from the insoluble parts. The supernatant was collected in a beaker, the pH was adjusted to 4.5 with 1 M HCl, and then it was centrifuged again under the same conditions to separate the precipitated proteins.

2.3. Drying processes

The precipitated proteins obtained after extraction from sesame cake were dried by three different drying processes, namely hot air drying (OD), spray drying (SD), and freeze-drying (FD). Parameters commonly used in the literature for drying proteins were preferred (Dabbour et al., 2021; Li et al., 2022; Nie et al., 2023). A hot-air oven (Miprolab, Türkiye) was used for OD, and the drying process was carried out at 55 °C with an airflow velocity of 1 m/s until the moisture content of the samples decreased to 5–6 %. A laboratory-scale spray dryer (B15, Unopex, İzmir, Türkiye) was used in the SD process. The drying process was carried out under an air inlet temperature of 150 °C, a feed flow rate of 9 mL/min, an airflow rate of 80 %, a nozzle diameter of 0.19 mm, and an outlet temperature of 80 °C. FD of sesame proteins was carried out using a freeze-dryer (Teknosem, Toros TRS-4/4, Türkiye) at −56 °C and 10^{-3} mbar pressure after the samples were frozen at −24 °C for 24 h. To get micro-sized protein powders, the dried samples using three different methods were ground using a coffee grinder.

2.4. Proximate composition

Moisture, ash, lipid, and protein content of the sesame seed protein isolates were determined according to AOAC procedures (AOAC, 2000) by gravimetric method at 105 °C, by incineration at 550 °C, by the Soxhlet method with petroleum ether, and by the Kjeldahl method with a conversion factor of 6.25, respectively.

2.5. Particle size distribution, polydispersity index (PDI) and zeta potential

Particle size distribution and PDI of sesame proteins in aqueous dispersions (4 %) were performed with a laser diffraction particle size-measuring device (Malvern Instruments, Mastersizer 3000 model, England). For measurement, sesame protein samples were diluted 1:100 in ultrapure water; the protein solutions were sonicated at 40 KHz for 5 min and then analyzed at 25 °C. To determine the zeta potential of sesame protein samples, protein samples were dispersed in distilled water to obtain a test solution (1 mg/mL). One mL of protein solution was injected into the zeta cell, and zeta potential was measured using Zetasizer Nano ZS90 (Malvern Instruments, Worcestershire, UK) in triplicate at 25 °C.

2.6. Gel electrophoresis (SDS-PAGE)

The molecular structures of sesame protein isolates were analyzed using sodium dodecyl sulfate-polyacrylamide gel electrophoresis (SDS-PAGE), which was performed according to the method reported by Laemmli (1970). The SDS-PAGE analyses used 12 % separating and 4 % stacking gels. Firstly, sesame protein stock solution (25 mg/mL) was mixed with buffer solution containing 0.125 M Tris-HCl buffer (pH 6.8), 4 % (*w/v*) SDS, 20 % (w/v) glycerol, and 0.5 % 2 2-mercaptoethanol at a 1:1 ratio, and 25 μL bromphenol blue was added. Then, the samples were kept in boiling water for 5 min, and after cooling, the samples (10 μL) were applied to the polyacrylamide gels placed in the electrophoresis tank. The electrophoresis process was started after the tank was filled with buffer solution (0.025 M Tris, 0.192 M glycine, and 10 % (w/v) SDS). Running voltages for the stacking and the separating gels were set to 100 and 110 *V*, respectively. The gels were kept in a staining solution containing 0.1 % Coomassie Brilliant Blue, 40 % methanol, and 7 % acetic acid overnight. Then they were kept in a destaining solution containing 40 % methanol and 7 % acetic acid for 4–5 h. The separated

protein bands were estimated by comparing molecular weights with a standard protein marker (Bio-Rad) with a 10–250 kDa molecular weight.

2.7. Color properties

The color values of sesame protein samples dried using different methods were determined using a colorimeter (Konica Minolta CM-5, Osaka, Japan), which was calibrated with a black and white ceramic plate. The CIELAB scale was used to evaluate the L^*, a^*, and b^* color values.

2.8. Fourier transform infrared spectroscopy (FTIR)

Possible changes in the chemical bond structures of proteins in powder form were monitored by FTIR (Perkin Elmer, Spectrum Two model, USA) analysis. For this purpose, powder samples were analyzed at a resolution of 4 cm^{-1} in the wavenumber range of 4000–650 cm^{-1}. The Amide *I* region was subjected to a self-deconvolution process to determine the effect of the different drying processes on the secondary structure content (α-helix, β-sheet, β-turn, and random coil). The Amide *I* band of samples was deconvoluted and fitted to a Gaussian model for quantification of secondary structural properties.

2.9. Surface hydrophobicity

The surface hydrophobicity of sesame protein samples was determined according to the method described by Arzeni et al. (2012). For this purpose, protein solution (0.4 mg/mL, pH 7.0) was prepared and centrifuged at 1000 *xg* for 10 min. Then, protein suspensions in the concentration range of 0.025–0.2 mg/mL were prepared, and the suspensions were incubated in a dark environment for 15 min at room temperature after the addition of 40 μL of 1-anilino-8-naphathalene-sulfonate (ANS) solution (2.4 mg/mL). After the suspensions were transferred to quartz cuvettes, their relative fluorescence intensities were recorded with a fluorescence spectrophotometer (FluoroMax-4, Horiba Scientific, Kyoto, Japan) at the excitation wavelength and the emission wavelength of 390 nm and 470 nm, respectively. Surface hydrophobicity values of sesame protein isolates were calculated by considering the initial slope of the relative fluorescence intensity (RFI) plot as a function of protein concentration (Eq. 1).

$$RFI = (F - F_0)/F_0 \quad (1)$$

where, F and F_0 refer to the reading of the protein-ANS conjugate and the protein-free ANS solution, respectively.

2.10. Free and total sulfhydryl (-SH) groups

The effect of different drying methods on the -SH groups of sesame protein was determined using the method reported by Ellman (1959). Sesame protein isolates were mixed with buffer solution (pH 7.0, prepared using 0.086 M Tris- (hydroxymethyl) aminomethane, 0.09 M glycine, and 4 mM ethylenediamine-tetra acetic acid disodium salt) to contain 0.2 % (*w/v*) protein and it was centrifuged at 8000 rpm at 4 °C for 15 min. Then, 0.03 mL of Ellman's solution (4 mg/mL 5′,5-dithiobis 2-nitrobenzoic acid, DTNB) was added to 3 mL of supernatant, the mixture was incubated at 20 °C in the dark for 15 min, and the absorbance measured at 412 nm wavelength by a UV–Vis spectrophotometer (Shimadzu, 1800, Japan) (H. Hu et al., 2013). In order to determine the total -SH groups, 6 M urea and 0.5 % (w/v) SDS were added to the buffer solution, and the above-mentioned procedures were applied exactly (Arzeni et al., 2012).

$$\mu MolSH/g = (73.53 x A_{412} x\, D)/C \quad (2)$$

where A_{412} refers to the absorbance at 412 nm; C refers to the protein concentration of the solution (mg/mL); and D refers to the dilution factor. The factor (73.53) is derived from the molar absorption constant of (10^6/ (1.36×10^4)).

2.11. Thermal properties

The thermal properties of sesame seed proteins obtained by different drying processes were evaluated with a differential scanning calorimeter (Metler Toledo, DSC-1 Star, USA). All samples were held in a desiccator containing silica for 1 week to remove moisture. The powdered protein samples (5–10 mg) were weighed into aluminum pans, sealed, and heated from 20 to 160 °C at a heating rate of 10 °C/min. An empty aluminum pan was used as a reference.

2.12. Techno-functional properties

The protein solubility of sesame protein isolates was determined using the method suggested by Klompong, Benjakul, Kantachote, and Shahidi (2007). For this purpose, protein suspension (0.01 g/mL) was prepared and centrifuged at 8000 rpm at 4 °C for 15 min. The absorbance of the mixture was read at a wavelength of 500 nm after the resulting supernatant was mixed with Biuret reagent at a ratio of 1:1. The protein amount of the supernatant was calculated using the bovine serum albumin standard curve, and the protein solubility was determined based on the total protein amount.

To determine the water- and oil-holding capacities of proteins, 0.1 g of the sample was mixed with 1 mL of water or 1 mL of oil in a tube of known tare, and the supernatant was removed by centrifugation at 1800 rpm for 20 min for water-holding and at 8000 rpm for 10 min for oil-holding capacities. After removing the supernatant, the tubes were weighed, and water- or oil-holding capacity was calculated from the weight difference as grams of water or oil absorbed per gram of protein, respectively.

For the determination of emulsifying properties, 30 mL of sesame protein solution (0.01 g/mL) was mixed with 10 mL of sunflower oil, and the mixture was homogenized at 15.000 rpm for 1 min. Immediately after the emulsion formed and 10 min later, 50 μL of the emulsion sample was mixed with 5 mL of 0.1 % SDS in a test tube, and the absorbance was read at 500 nm using a UV-VIS spectrophotometer. Emulsion capacity and stability were calculated using the following equations.

$$Emulsion\ capacity = \frac{2x2.303xA_0}{0.25xm} \quad (3)$$

$$Emulsion\ stability = \frac{A_{10}x\Delta t}{\Delta A} \quad (4)$$

where A_0 and A_{10} refer to the absorbance at 0 min and 10 min, respectively, m refers to the amount of protein (g), $\Delta t = 10$ min, and ΔA refers to the difference between the initial absorbance and absorbance after 10 min.

To determine the foam capacity and stability of samples, 0.3 g of protein sample was transferred to a 100 mL measuring cylinder, mixed with 30 mL of distilled water, and homogenized with Ultra-Turrax at 14.000 rpm for 3 min. The volume was recorded immediately after homogenization and 30 min later. The foam capacity and stability of protein samples were calculated using the following equations:

$$Foam\ capacity\ (\%) = \frac{V_2 - V_1}{V_1} \quad (5)$$

$$Foam\ stability\ (\%) = \frac{V_3 - V_1}{V_1} \quad (6)$$

where V_1, V_2, and V_3 refer to the volume (mL) of protein dispersion before and after homogenization, and after 30 min of storage, respectively.

2.13. Rheological properties

The flow properties of sesame proteins were determined with a rheometer device (Anton Paar, MCR 302 model, Austria) with a 2° conical angle and 25 mm diameter, conical-plane geometry, at 25 ± 0.1 °C. For this purpose, suspensions containing 4 % protein were subjected to steady shear rheological analysis for 300 s at a shear rate ranging from 0 to 100 1/s.

Dynamic rheological tests were carried out to determine the viscoelastic properties of sesame proteins. For this purpose, a suspension was prepared with distilled water containing 4 % protein, and stress sweep analysis was performed in the range of 0.01–10 Pa and at a constant frequency of 0.681 rad/s to determine the linear viscoelastic region (LVR). Then, frequency sweep analysis was performed in the range of 0.681–46.42 rad/s in the determined LVR (defined as 0.2 Pa). Measurements were carried out at a temperature of 25 ± 0.1 °C.

2.14. In vitro digestibility

In vitro static digestibility (IVD) of sesame protein isolates was performed according to the COST consensus method (Minekus et al., 2014). Protein suspensions were prepared with distilled water containing 4 % protein and stirred at room temperature for 1 h. To simulate oral digestion, 200 μL of protein suspension was mixed with 7 mL of salivary fluids (pH 7.0), 1 mL of α-amylase solution (75 U/mL), 25 μL of 0.3 mol/L $CaCl_2$, and 0.975 μL of distilled water to reach a final volume of 9 mL. The mixture was incubated in a shaking water bath at 37 °C for 2 min. To simulate gastric digestion, 7.5 mL of gastric fluid, 1.6 mL of pepsin solution (2000 U/mL), 5 μL of 0.3 mol/L $CaCl_2$ was added to the mixture; the pH of the mixture was adjusted to 3.0 using 1 mol/L HCl, and the mixture was incubated in a shaking water bath at 37 °C for 2 h. After simulated gastric digestion, 2 mL was taken for each sample.

To simulate intestinal digestion, the rest of the mixture was mixed with 11 mL of intestinal fluid, 5 mL of pancreatin (100 U/mL), 2.5 mL of 160 mmol/L bile, and 40 μL of 0.3 mol/L $CaCl_2$, and the pH of the mixture was adjusted to 7.0 using 1 mol/L NaOH. The mixture was incubated in a shaking water bath at 37 °C for 2 h. After simulated intestinal digestion, 2 mL of sample was retaken for each sample. The in vitro digestibility of the proteins based on the peptide concentration was calculated according to the following equation:

$$IVD(\%) = \frac{VxnxC}{M}x100 \quad (7)$$

where V refers to the volume of digestion (mL), n refers to the dilution factor, M refers to the mass of the protein (mg), and C refers to the concentration of peptides released (mg/mL) following the deduction of a blank (buffer and digestive enzymes).

The peptide concentration was determined using the Lowry method (Waterborg, 2009). For this, 0.5 mL of sample was mixed with 2.5 mL of Lowry solution, and the mixture was left at room temperature for 10 min. Then, 0.25 mL of Folin-Ciocelteu phenol solution was added and incubated in the dark for 30 min. Finally, the absorbance of the samples was measured using a spectrometer at 750 nm. The amount of soluble protein was calculated using the bovine serum albumin standard curve.

2.15. Statistical analysis

All the measurements were carried out in triplicate, and the results are given as mean ± standard deviation. Statistical data evaluation was done using the SPSS Statistics 21.0 program (SPSS Inc., Chicago, Illinois, USA). The results of the analysis were subjected to a one-way analysis of variance (ANOVA), and the difference between the means was determined by the Duncan multiple comparison test ($P < 0.05$). Rheological results were evaluated with the rheometer's software package (Anton-Paar, Rheo Compass v1.21, Austria).

3. Results and discussion

3.1. Proximate composition and color properties

The proximate composition of sesame protein isolates (SPI) produced using hot air drying (OD), spray drying (SD), and freeze drying (FD) is presented in Table 1. The moisture content ranged from 2.58 % to 3.39 %, while ash content varied between 0.93 % and 1.05 %. No significant differences ($P > 0.05$) were observed in either moisture or ash content among the different drying methods. Similarly, oil content did not differ significantly across the samples ($P > 0.05$), suggesting that the drying technique had minimal impact on the overall fat retention of the protein isolates.

Regarding protein content, FD-PI exhibited the highest value (91.34 %), followed by SD-PI (90.71 %) and OD-PI (90.52 %). Although these differences were not statistically significant ($P > 0.05$), the slight variations may be attributed to the influence of drying temperature and exposure time during processing. These findings are consistent with those reported by Joshi, Adhikari, Aldred, Panozzo, and Kasapis (2011), who studied lentil protein isolates prepared using various drying techniques. Their results also indicated that while drying processes can alter the physical structure of protein granules, they induce only partial changes to the chemical composition (Joshi et al., 2011).

Color attributes (L^*, a^*, b^*) of OD-PI, SD-PI, and FD-PI were measured and found to range from 70.99 to 83.19 (L^*), 4.18–6.73 (a^*), and 17.19–23.07 (b^*), respectively (Table 1). Statistically significant differences ($P < 0.05$) were observed among the three drying methods. SD-PI showed the highest L^* (lightness) and the lowest a^* (redness) and b^* (yellowness) values, indicating a lighter and less pigmented powder. Conversely, OD-PI exhibited the lowest L^* value, suggesting a darker, more brownish appearance.

These findings align with a previous study on mung bean protein isolate powder, where spray drying resulted in a brighter product compared to oven drying (Brishti et al., 2020). Several factors contribute to the color of protein powders, including inherent protein characteristics, pigment concentration, protein purity, and pigment removal efficiency during processing (Shen et al., 2021).

Spray drying typically produces smaller, more uniformly distributed particles with a larger surface area. This increased surface area can lead to surface coating by protein layers that mask the underlying color pigments, resulting in a white powder appearance (Li et al., 2022). In contrast, the darker color observed in OD-PI may result from the formation of melanoidins—brown-colored compounds produced via Maillard reactions between amino groups and carbonyl compounds under heat exposure during oven drying (Brishti et al., 2020). Additionally, prolonged oxygen exposure during the OD process could contribute to protein oxidation, further leading to discoloration and a less desirable appearance.

Table 1
Proximate composition and color properties of sesame seed protein isolates fabricated by different drying methods.

Parameters	OD-PI	SD-PI	FD-PI
Moisture content (%)	3.39 ± 0.59^a	2.58 ± 0.61^a	3.09 ± 0.42^a
Ash content (%)	1.03 ± 0.09^a	0.93 ± 0.07^a	1.05 ± 0.09^a
Oil content (%)	0.98 ± 0.08^a	1.03 ± 0.06^a	0.99 ± 0.06^a
Protein content (%)	90.52 ± 0.64^a	90.71 ± 0.42^a	91.34 ± 0.57^a
Color properties			
L^*	70.99 ± 0.69^b	83.19 ± 0.19^a	72.09 ± 0.30^b
a^*	6.42 ± 0.13^b	4.18 ± 0.26^c	6.73 ± 0.05^a
b^*	20.69 ± 0.56^b	17.19 ± 0.48^c	23.07 ± 0.19^a

OD-PI: hot air dried sesame protein isolate; SD-PI: spray dried sesame protein isolate; FD-PI: freeze-dried sesame protein isolate. The superscript letters in the same row show statistical significance among the drying methods ($p < 0.05$).

3.2. Particle size, PDI, zeta potential and gel electrophoresis

The physicochemical, reconstitution, and techno-functional properties of proteins—critical to their applicability in food systems—are significantly influenced by particle size. Beyond functionality, particle size analysis also offers insight into conformational changes and the degree of protein aggregation (Ye et al., 2024). Fig. 1 presents the particle size distribution, average particle size, PDI, and zeta potential of SPI processed using different drying techniques. As shown in Fig. 1a, spray-dried SPI (SD-PI) exhibited a unimodal distribution within the 2.1–6.6 μm range, whereas both oven-dried (OD-PI) and freeze-dried (FD-PI) samples showed prominent bimodal distributions ranging from 0.05 to 0.5 μm and 4.1–13.7 μm. The unimodal, narrower distribution observed in SD-PI indicates better dispersion behavior in water, which is favorable for many food formulations. This finding is consistent with prior studies highlighting that spray drying produces more uniform and smaller particles (Shen et al., 2021). Fig. 1b further confirms that SD-PI had the lowest average particle size (4.51 μm), followed by OD-PI (11.51 μm) and FD-PI (18.16 μm), with differences being statistically significant ($P < 0.05$). The smaller particle size observed in SD-PI may be attributed to the rapid drying process at high temperatures and short residence times, which minimizes protein denaturation and aggregation (Ye et al., 2024). In contrast, OD-PI and FD-PI required post-drying grinding to reduce particle size, and the nature of the drying process may have facilitated aggregation. Specifically, the larger particle size in OD-PI could result from the formation of insoluble, crystalline aggregates under prolonged heating conditions (Lin et al., 2020). Meanwhile, the freeze-concentration phenomenon during FD may have increased molecular interactions—such as electrostatic and hydrophobic forces—leading to greater protein aggregation and ultimately larger particles (Gong et al., 2016).

The PDI provides insight into particle homogeneity, where lower values indicate a more uniform particle size distribution. In this study, PDI values ranged from 0.19 to 0.28 across all samples (Fig. 1b), with SD-PI exhibiting the lowest PDI, suggesting a more uniform and homogeneous protein dispersion. Although all samples were classified as polydisperse (since PDI > 0.1), their PDI values remained below 0.3, indicating stable dispersions (Wang, Niu, et al., 2022). Such stability is critical in product formulations requiring consistent solubility and emulsification.

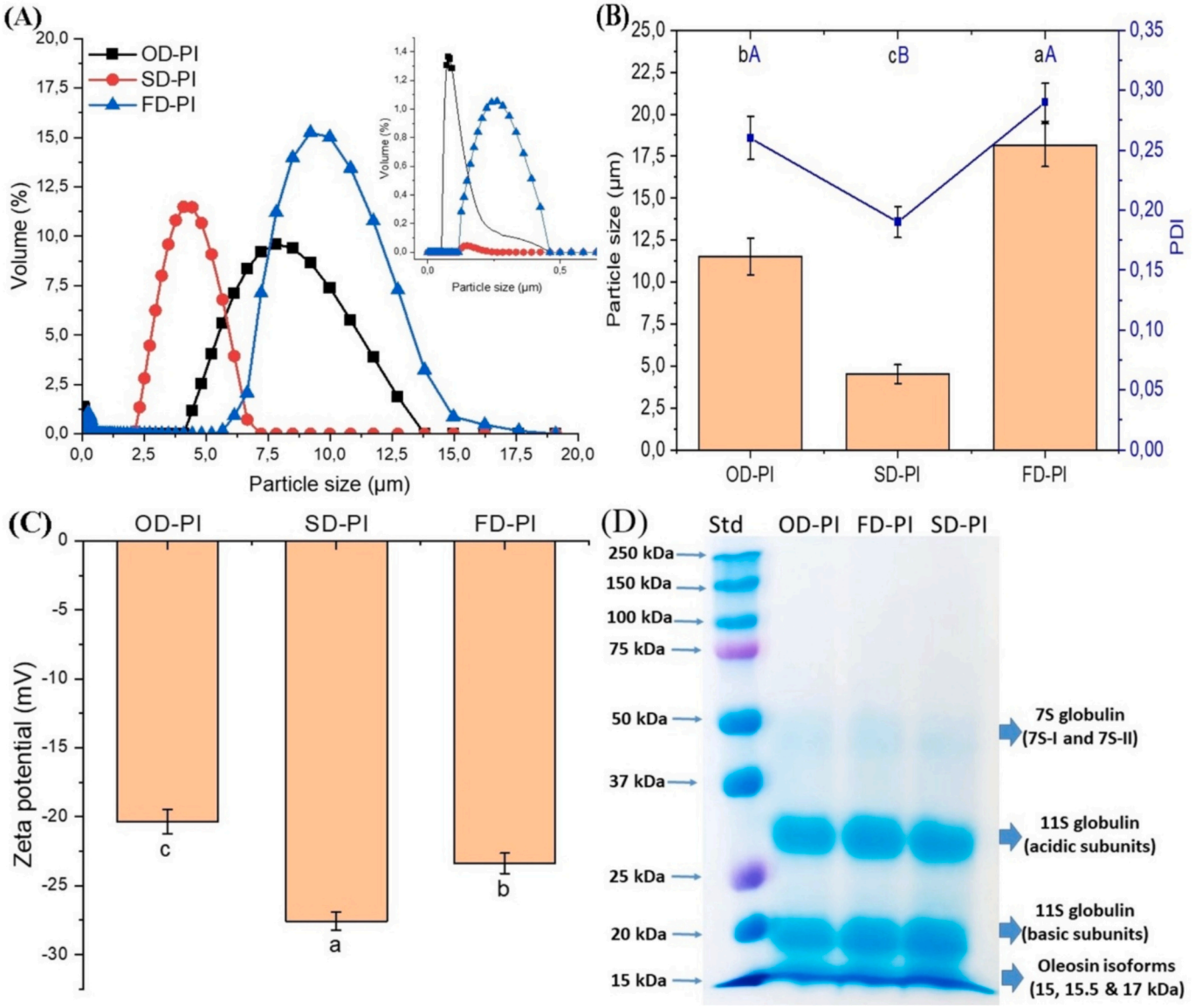

Fig. 1. The particle size distribution (a), average particle size, PDI (b) and zeta potential (c) of the sesame protein isolates dried with different drying techniques (OD-PI: hot air dried sesame protein isolate; SD-PI: spray dried sesame protein isolate; FD-PI: freeze-dried sesame protein isolate).

Zeta potential, a key indicator of colloidal stability, measures the net surface charge of dispersed particles. Higher absolute zeta potential values reflect greater electrostatic repulsion between particles, which reduces aggregation and promotes dispersion stability. As shown in Fig. 1c, all protein samples exhibited negative zeta potentials, indicating negatively charged protein surfaces. SD-PI had the highest absolute value (−27.58 mV), followed by FD-PI (−23.39 mV) and OD-PI (−20.36 mV). The greater zeta potential in SD-PI may be attributed to partial unfolding of proteins during spray drying, which exposes more charged amino acid residues to the surface. Conversely, the larger particle sizes in OD-PI and FD-PI, resulting from aggregation, likely contributed to the reduced surface charge due to limited exposure of charged residues.

Interestingly, the trend in zeta potential closely mirrored that of surface hydrophobicity. This relationship is consistent with the findings of Li et al. (2022), who noted that an increase in the absolute value of zeta potential corresponded with higher surface hydrophobicity. This behavior may stem from structural rearrangements that bring hydrophobic regions to the surface during drying. A protein's high surface hydrophobicity indicates the presence of hydrophobic groups on the surface, which is associated with increased stability of the protein solution in water and, consequently, high electrostatic repulsion. This high electrostatic repulsion results from the high isotropic charge on the protein's surface and indicates a high absolute value of the protein's zeta potential. Importantly, zeta potential values exceeding ±20 mV are typically considered sufficient to confer electrostatic stability through repulsion, reducing the risk of aggregation. Taken together, these results emphasize that spray drying offers significant advantages in terms of producing uniformly sized, well-dispersed, and electrostatically stable sesame protein particles. Such characteristics are highly desirable for enhancing protein solubility, emulsification, and dispersion in food applications, making SD a preferred method for preserving the techno-functional integrity of SPI.

SDS-PAGE was used to assess the alterations in the protein composition of SPI. Fig. 1d revealed that sesame protein isolates dried using different drying technologies showed different subunits with molecular weights ranging from approximately 15 to 50 kDa. 7S globulin (1–2 %) subunits with a molecular weight of roughly 50 kDa were found in the samples. Additionally, 12S globulin's basic and acidic subunits were detected in the 15–37 kDa band range. In contrast, polypeptide bands with a molecular weight of roughly 15 kDa are assumed to represent different isoforms of oleosin (Achouri, Nail, & Boye, 2012; Baskinci and Gul, 2023). As shown in Fig. 1d, all SPI showed the same band pattern despite the various drying methods, suggesting that drying procedures do not result in the quaternary structural separation of mung bean protein subunits. This agrees with Brishti et al. (2020) and Qiang Zhao et al. (2013), who indicated that different drying techniques did not affect the subunit constituents of mung bean and rice protein isolates, respectively.

3.3. FTIR

FTIR spectroscopy was utilized to investigate the secondary structure of protein isolates and the effect of the drying techniques on protein fractions' conformational components. The protein samples' original FTIR spectra and secondary structures modeled with a Gaussian function are given in Fig. 2. As shown in Fig. 2a, infrared spectra of protein molecules display a wide range of vibrational frequencies. The band at 3280 1/cm was associated with the hydrogen bond formed between the protein and water or other organic chemicals (Nan et al., 2018). The bands at 2924 1/cm and 2854 1/cm were assigned to C—H and N—H stretching (Amide *B*), respectively. Amide *I*, II, and III regions are the primary bands that display the structure-specific fingerprints of proteins. In all samples, the Amide *I* band (at 1627 1/cm) was assigned to the C—O stretching vibration of the peptide backbone, which is extensively employed in investigating secondary structures in proteins. The Amide II band (at 1528 1/cm) was assigned to N—H bending and C—N

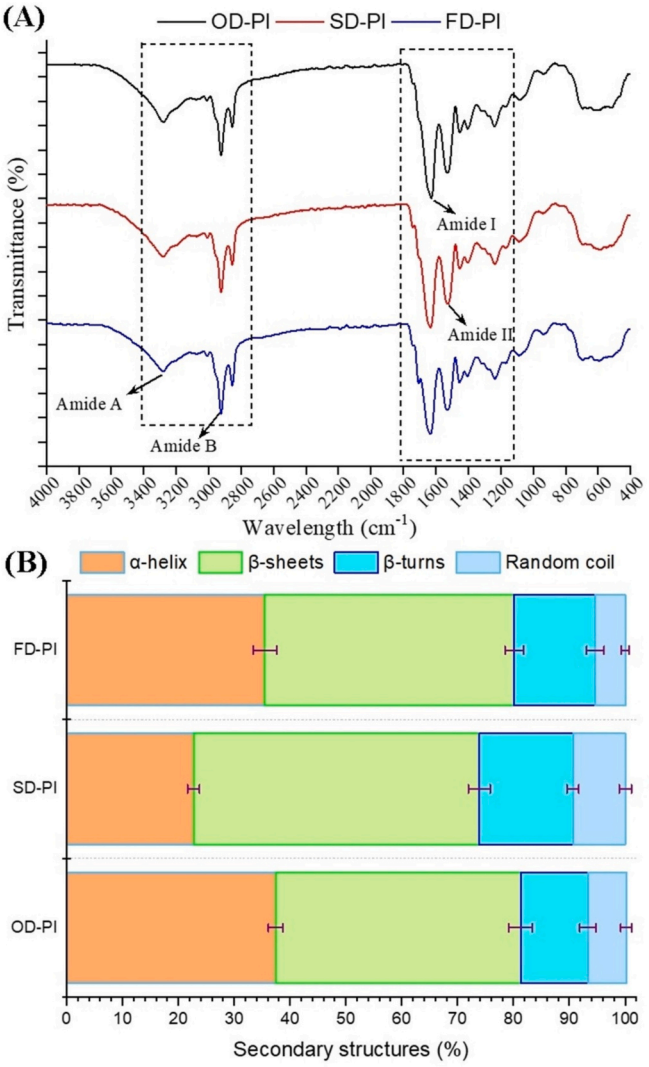

Fig. 2. FTIR spectra (a) and secondary structures (b) of the sesame protein isolates dried with different drying techniques (OD-PI: hot air dried sesame protein isolate; SD-PI: spray dried sesame protein isolate; FD-PI: freeze-dried sesame protein isolate).

stretching vibrations, and N—H rotational vibrations and C—N stretching were linked to the amide III band (De Maria, Ferrari, & Maresca, 2016). Even though the protein samples' FTIR spectra do not differ significantly, a closer look at the amide I band reveals details about the proteins' secondary structures because each secondary structural element in the protein has a strong correlation with the frequencies of the amide I region components out of all the regions. Different protein secondary structures, including the α-helix (1650–1660 1/cm), β-sheets (1610–1642 1/cm), β-turns (1660–1680 1/cm), and random coils (1642–1650 1/cm), are identified by the various wavelength ranges recorded in this region (Barth, 2007). According to the findings, sesame seed proteins had a higher percentage of β-sheets than α-helices, just like the majority of other plant proteins (Ye et al., 2024). As shown in Fig. 2b, the secondary structure of the sesame protein isolate was significantly influenced by different drying techniques ($P < 0.05$). The β-sheets content of SD-PI (51.14 %) was higher than those of FD-PI (44.66 %) and OD-PI (43.86 %), indicating that SD-PI had a more organized structure than other samples (Mune Mune, Sogi, & Minka, 2017). This result is consistent with the DSC findings, showing that SD-PI has the highest denaturation ΔH, meaning it takes the most energy to denature due to its highly organized, compact structure (Brishti et al., 2020). However, it did not coincide with the water

solubility findings of protein samples. Mune Mune et al. (2017) stated that protein solubility increases with increasing unordered structure proportion and decreases with rising β-sheets proportion. High solubility is observed at combined high unordered and low β-sheets secondary structures. At the same time, solubility is related to particle size and, consequently, particle surface area. As particle size decreases, hydrogen bonding and electrostatic interactions increase, increasing protein-water interaction. Therefore, we can say that smaller particle size, rather than higher β-sheet content, impacts SD-PI solubility. On the other hand, the rise in the percentage of random coils (9.39 %) indicated that some of the α-helix structures in SD-PI changed into random coils. This is probably due to the partial unfolding of secondary structures of SD-PI during drying. The high random coil as an unordered structure improved in the digestibility of proteins because it is easily accessible by gastrointestinal enzymes during digestion (Brishti et al., 2020). The β-turn contents of the samples were between 12.06 % and 17.53 %, and SD-PI had the highest β-turn secondary structure ($P < 0.05$). Protein molecules' partial unfolding and increased proportion of β-turn secondary structure increased the flexibility of proteins, which in turn promoted protein rearrangement at the oil-water interface and inhibited coalescence (Mune Mune et al., 2017).

3.4. Free and total -SH groups and surface hydrophobicity (H0)

Sulfhydryl groups (SH) are crucial for protein structure and have been widely identified as essential functional groups in various proteins. The content of free and total -SH groups of protein samples are exhibited in Table 2. Free -SH groups of the samples ranged between 4.66 and 5.44 μmol/g, and no significant difference between the samples was detected ($P > 0.05$). However, the numerically highest free –SH group was detected in FD-PI, followed by the SD-PI and OD-PI. The low temperature and high vacuum used for freeze drying may be the reason for the reduced loss of sulfhydryl groups in the FD-PI (X.-Z. Hu et al., 2010). The notable loss of free -SH group in OD-PI could be explained by the creation of protein aggregates because of the intermolecular disulfide bonds of sesame protein isolate under OD conditions, which include a comparatively higher temperature and longer time (Nikoo, Benjakul, & Xu, 2015). Also, sesame protein isolates were more vulnerable to oxidation when exposed to oxygen because OD did not eliminate oxygen, resulting in a decrease in the free -SH group (Wang, Niu, et al., 2022). Lin et al. (2020) found similar results in the drying of phosphorylated Antarctic krill protein by different drying techniques, and they stated that the hot-air samples had the lowest content of SH, probably due to prolonged high-temperature drying of the hot-air dried sample might have facilitated the oxidation of the sulfhydryl group. Moreover, higher temperature but shorter drying duration was applied to the SD-PI; therefore, the free -SH group may be lost more in OD-PI than SD-PI.

Table 2
-SH content, H_0 and techno-functional properties of sesame seed protein isolates fabricated by different drying methods.

Parameters	OD-PI	SD-PI	FD-PI
Free –SH group (μMol SH/g)	4.66 ± 0.30^{a}	4.88 ± 0.26^{a}	5.44 ± 0.40^{a}
Total –SH group (μMol SH/g)	23.38 ± 0.99^{a}	23.73 ± 1.74^{a}	21.27 ± 0.65^{a}
Surface hydrophobicity (H_0)	21.62 ± 2.41^{b}	27.13 ± 1.09^{a}	29.03 ± 1.13^{a}
Solubility (%)	48.49 ± 0.96^{c}	72.62 ± 6.82^{a}	55.82 ± 1.68^{b}
Emulsion capacity (%)	27.24 ± 0.80^{a}	29.91 ± 1.04^{a}	25.86 ± 1.27^{b}
Emulsion stability (min)	39.35 ± 1.33^{c}	64.83 ± 5.20^{a}	51.69 ± 4.15^{b}
Foaming capacity (%)	109.17 ± 7.39^{b}	127.78 ± 9.62^{a}	79.17 ± 8.33^{c}
Foaming stability (%)	32.50 ± 4.19^{b}	47.78 ± 6.94^{a}	27.50 ± 4.19^{b}
Water holding capacity (%)	1.73 ± 0.05^{b}	1.81 ± 0.03^{a}	1.71 ± 0.05^{b}
Oil holding capacity (%)	1.35 ± 0.06^{b}	1.57 ± 0.05^{a}	1.61 ± 0.03^{a}

OD-PI: hot air dried sesame protein isolate; SD-PI: spray dried sesame protein isolate; FD-PI: freeze-dried sesame protein isolate. The superscript letters in the same row show statistical significance among the drying methods ($p < 0.05$).

The total -SH group ranged from 21.27 to 22.73 μmol/g, and there was no significant difference among all the drying methods ($P > 0.05$; Table 2), corroborating previous research findings (Shen et al., 2021). Even so, the total -SH group in OD-PI and SD-PI was slightly higher than that of FD-PI. Similarly, Brishti et al. (2020) also concluded the same conclusion, citing a higher total -SH group in the samples dried with oven and spray drying compared to freeze-dried samples. This may be because of increased protein denaturation under a heated environment, which causes the protein structure to unfold and more -SH groups to be visible in the oven and spray-dried samples (Brishti et al., 2020). The different degrees of protein denaturation can result from low-temperature stress, freezing stress, including phase separation, and drying stress during freeze-drying (Lin et al., 2020), resulting in more loss in the total -SH group in FD-PI compared to the SD-PI and OD-PI.

Protein surface hydrophobicity (H0) indicates the degree of exposure of hydrophobic amino acids on the surface of protein molecules, which determines proteins' techno-functional properties, including solubility, emulsifying and foaming properties (Li et al., 2022; Tang & Jiang, 2007). The two primary factors that contribute to surface hydrophobicity are the slight denaturation of proteins through heating, freezing, and other processes, which increases surface hydrophobicity by exposing hydrophobic regions and unfolding the structure, and the aggregation of proteins through protein-protein interactions, which decreases surface hydrophobicity by reducing exposed hydrophobic regions (X.-Z. Hu et al., 2010; Petruccelli & Añón, 1996)). It can be seen from Table 2 that the H0 values were different, with a similar order as follows: FD-PI>SD-PI>OD-PI. No statistical difference was found between FD-PI and SD-PI samples regarding the H0 value. Similar results were reported by (X.-Z. Hu et al., 2010), with the highest H0 value recorded for freeze-dried soy protein, followed by spray-dried and vacuum oven-dried samples. This finding is also reported by Shen et al. (2021) and Brishti et al. (2020), who stated that the freeze-dried quinoa proteins exhibited the highest H0 value, probably attributing to a certain extent of denaturation occurred in the freeze-dried sample by exposing hydrophobic regions. On the other hand, because of the hydrophobic interchange process between the protein molecules, the protein dried by OD underwent more intense denaturation. This was also linked to creating a film on the protein surface, which led to protein aggregation (through protein-protein interactions) and low surface hydrophobicity (Deak & Johnson, 2006; X.-Z. Hu et al., 2010). Moreover, the degree of protein oxidation may cause variations in surface hydrophobicity.

3.5. Thermal properties

Differential scanning calorimetry (DSC) is frequently used to determine the characteristics of thermal transitions in macromolecules and to evaluate the impact of various drying techniques on the denaturation, structural, and conformational changes of macromolecules (Lin et al., 2020). The DSC thermograms of samples are presented in Fig. 3, and the thermal parameters, including onset temperature (T_0), denaturation temperature (T_d), denaturation end temperature (T_3), and enthalpy (ΔH), are summarized in Table 3. All three sesame protein isolate samples showed a single endothermic peak with peak denaturation temperatures between 75 and 85 °C during the thermal scans from 20 to 120 °C, which was attributed to protein denaturation. The T0 values for OD-PI, FD-PI, and SD-PI were 45.06, 45.26, and 48.44 °C, respectively. The Td for these three protein samples was 81.83, 77.09, and 78.77 °C. T_d values for SD-PI and FD-PI were not significantly different ($P > 0.05$) and considerably lower than that of OD-PI ($P < 0.05$), indicating that OD-PI had higher thermal stability. The findings revealed comparable trends to those of Lin et al. (2020). Protein thermal stability is

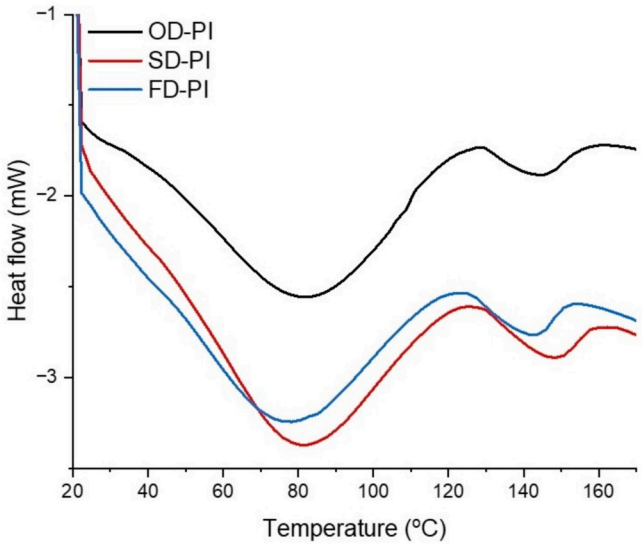

Fig. 3. DSC spectra of the of the sesame protein isolates dried with different drying techniques (OD-PI: hot air dried sesame protein isolate; SD-PI: spray dried sesame protein isolate; FD-PI: freeze-dried sesame protein isolate).

Table 3
Thermal properties of sesame seed protein isolates fabricated by different drying methods.

Samples	T_0 (°C)	T_d (°C)	T_{end} (°C)	ΔH (J/g)
OD-PI	45.06 ± 1.12b	81.83 ± 0.36a	112.55 ± 2.18a	28.86 ± 1.03c
SD-PI	48.44 ± 1.02a	78.77 ± 0.39b	106.62 ± 3.41b	33.25 ± 0.17a
FD-PI	45.26 ± 0.12b	77.09 ± 0.95b	108.1 ± 3.85b	30.4 ± 0.31b

OD-PI: hot air dried sesame protein isolate; SD-PI: spray dried sesame protein isolate; FD-PI: freeze-dried sesame protein isolate. T_0: onset temperature of denaturation; T_d: thermal denaturation temperature; T_{end}: end temperature of denaturation; ΔH: the enthalpy change of the endotherm. The superscript letters in the same column show statistical significance among the drying methods ($p < 0.05$).

demonstrated by T_d, where a higher T_d denotes more stability. This might happen because FD-PI has more heat-sensitive structures, such as α-helixes. Furthermore, the highest T_d results from a greater likelihood of the Maillard reaction in OD-PI via covalent bonding (Feyzi et al., 2018). As in T_d, the highest Tend value was determined in the OD-PI sample ($P < 0.05$), and the T_{end} values of SD-PI and FD-PI samples were similar ($P > 0.05$). The ΔH value was found to be much higher in SD-PI (33.25 J/g) than in FD-PI (30.4 J/g) and OD-PI (28.86 J/g) ($P < 0.05$). The energy required to denature the protein is shown by ΔH, which is the net energy value needed to break hydrophobic interactions (exothermic) and hydrogen bonds (endothermic) and correlates with the degree of ordered structure within proteins. The lower ΔH value in the OD-PI sample could be attributed to the higher protein denaturation during drying and the low ordered structure of the protein, reflecting the amorphous structure of the OD-PI sample. Long drying times during OD can denature many protein samples, making them particularly heat labile. The compact structure of the OD-PI sample was lost due to the disruption of many intermolecular bonds, and the energy needed for the complete denaturation decreased (Lin et al., 2020). From the result presented, the differences in ΔH of the samples were consistent with the H_0 results. OD-PI had the lowest ΔH, indicating the highest denaturation and protein conformational change; the OD-PI thus displayed the lowest H_0 value. High temperatures employed in the OD process may cause protein aggregation (via protein-protein interactions), which could reduce exposed hydrophobic regions and, in turn, H_0.

3.6. Techno-functional properties

Solubility is a crucial necessity for proteins to execute various techno-functional properties like emulsification and foaming in the food system, which is typically influenced by the proteins' hydrophobic/hydrophilic balance, depending on the denaturation and amino acid content of proteins and the thermodynamics of its interaction with water (dos Santos, Martins, Salas-Mellado, & Prentice, 2011; Ghribi et al., 2015). As seen in Table 2, solubility levels were 48.49–72.62 %, and the highest and lowest solubility were recorded for the SD-PI and OD-PI, respectively ($P < 0.05$). Joshi et al. (2011) reported that the drying process had a significant effect on the solubility of the lentil protein and informed that SD and FD protein samples showed higher solubility (81 % and 78 %, respectively) than that of the vacuum-dried samples (50 %). X.-Z. Hu et al. (2010) also reported similar results for the soy protein isolates, and solubility levels were 70.2 % and 40.8 % for SD and FD protein samples, respectively. Similarly, Shen et al. (2021) also investigated the effects of the drying process on the solubility of quinoa protein isolates, and they revealed that the solubility levels were 95.3 %, 93.7 % and 61.3 % for the SD, FD, and vacuum-dried (VD) protein samples, respectively. The high solubility performance of the protein samples dried by the spray drying process is attributed to the less denaturation and uniform and small particle size distribution compared to the oven drying process (Joshi et al., 2011). This could be because the study's dryer outlet temperature of approximately 85 °C is significantly lower than denaturation temperature of the sesame protein isolate. It was also reported that the SD proteins are produced in a very short time compared to FD and OD proteins, positively effecting the moisture evaporation performance. The significant denaturation of protein brought on by the OD process over and extended heating period may be the reason for the lower solubility of the OD-PI, which was in line with findings by Li et al. (2022). This denaturation may promote hydrophobic interactions between protein molecules, which result in the formation of a surface moisture barrier of the protein, decreasing in solubility (Shen et al., 2021). The ΔH values of all the samples in the current study showed that the SD-PI sample had the lowest protein denaturation, while the OD-PI had the highest protein denaturation, indicating that SD-PI had the highest solubility, while the OD-PI had the lowest solubility.

Emulsion capacity and stability values play an indispensable role in the food industry, representing the ability of protein to promote emulsion formation and maintain emulsion stability within a certain period. Table 2 shows the emulsion capacity values of the protein samples ranged between 25.86 and 29.91 m^2/g, while the emulsion stability values were in the range of 39.35–64.83 min. Notably, the emulsion capacities of SD-PI and OD-PI were statistically similar and both higher than FD-PI. Whereas, the lowest emulsion stability value was measured for OD-PI, which could be attributed to its lower protein solubility, as previously noted (X.-Z. Hu et al., 2010). A result similar to this was observed by Ye et al. (2024), who reported that the spray drying resulted in higher emulsifying properties. In general, hydrophobic interactions predominate at the oil-water interface, and the emulsifying capabilities are significantly impacted by the exposure of non-polar hydrophobic residues at the interface. Stronger emulsifier-oil droplet interaction and improved protein emulsifying capabilities can result from comparatively increased surface hydrophobicity (Gong et al., 2016). Emulsion stability is influenced by particle size and rheological properties of the emulsion; the smaller particle size led to better emulsion stability (Wang, Niu, et al., 2022). Considering the particle size, surface hydrophobicity and solubility of the SD-PI, a positive correlation was observed in the present study.

Another essential protein functionality concerning protein application in the food industry is foaming properties, which are determined by foaming capacity and foaming stability. While foaming capacity that denotes an ingredient's capacity to promote foam production, is related to the solubility, conformational chain flexibility, and the degree of

hydrophobicity of protein, foaming stability that denotes an ingredient's performance in keeping the foaming system stable over time, is influenced by proteins' rheological behavior, interactions with other proteins, pH, and temperature (Dong, Woo, & Quek, 2024). The foaming capacity and stability values were 79.17–127.78 % and 27.50–47.78 %, respectively (Table 2). Like the emulsion capacity and stability, SD-PI showed the highest foaming capacity and stability values, while the FD technique revealed the lowest foaming performance compared to other drying approaches. Ye et al. (2024) also reported that *Cinnamomum camphora* seed kernel protein isolate dried by SD showed the highest foaming capacity and stability due to its smallest particle size and maximum solubility. Higher solubility of proteins interacts with water molecules, quickly diffuses to the gas-liquid interface, and creates a protein-binding layer, resulting in better foaming capacity and stability (Qiaoli Zhao, Wang, Hong, Liu, & Li, 2021). Smaller protein particles, like those from SD, may be absorbed on the gas-liquid interface more quickly during whipping, generating more foam volume (Qiang Zhao et al., 2013). To create interfacial barriers around the air bubbles, proteins must be sufficiently unfolded and molecularly flexible (Aluko & Monu, 2003). Heating pretreatment also improved foaming capabilities, and partial protein unfolding helped to enhance foaming ability (Mune & Sogi, 2015). On the other hand, the FD-PI with the largest particle sizes may be absorbed the slowest during stirring to generate more foam (Wang, Niu, et al., 2022).

Water-holding capacity is a key parameter in determining proteins' solubility, swelling, gelation properties as well as water retention functionality, and oil-holding capacity describes the ability of the protein to hold and retain an amount of added oil, all of which have an impact on the texture and quality of food. As shown in Table 2, the water-holding capacity of the protein samples ranged between 1.71 % and 1.81 %, and SD-PI showed higher water-holding capacity ($P < 0.05$) compared to the other samples that had no statistical difference between them ($P > 0.05$). The higher water-holding capacity in the SD-PI could be due to its finer particle size and larger specific surface area (Shen et al., 2021). Furthermore, losses of soluble proteins and higher availability of polar amino acids contribute to the water-holding capacity of proteins (Ghribi et al., 2015). Our result agreed with Shen et al. (2021) who indicated that spray-dried quinoa protein isolate exhibited relatively better water-holding capacity than the proteins from the other methods. Similarly, Özdemir, Görgüç, Gençdağ, and Yılmaz (2022) stated that the water-holding capacity of protein isolate from sesame bran dried by spraying drying is significantly higher than that of protein dried by freeze-drying.

The oil-holding capacity of SD-PI (1.57 %) was somewhat higher than that of OD-PI (1.35 %), whereas FD-PI's oil-holding capacity (1.61 %) was noticeably greater than both of the previous two (Table 2), according to an earlier study (Özdemir et al., 2022). However, no significant difference between SD-PI and FD-PI samples regarding oil-holding capacity was observed ($P > 0.05$). The higher oil-holding capacity of FD-PI could be due to its hollow cavity and fluffy porous structure, which may physically capture more oil molecules during centrifugation (Brishti et al., 2020; Ghribi et al., 2015). The enhanced hydrophobic properties may explain the high oil-holding capacity of SD-PI, the interception retention of physical structure, and the better fat-binding ability of the non-polar amino acid (Lin et al., 2020).

3.7. Rheological properties

Fig. 4 illustrates the rheological properties of the sesame seed protein isolated as affected by different drying techniques. As seen in Fig. 4a, all protein samples showed pseudoplastic flow behavior in which the apparent viscosity decreased dramatically with the increase in shear rate level from 0 to 100 1/s shear rate. A possible explanation is the reduction of viscosities caused by the deformation and rupture of the aggregated network of protein suspensions with shear rate. Additionally, this is mainly associated with the orientation of particles and molecules due

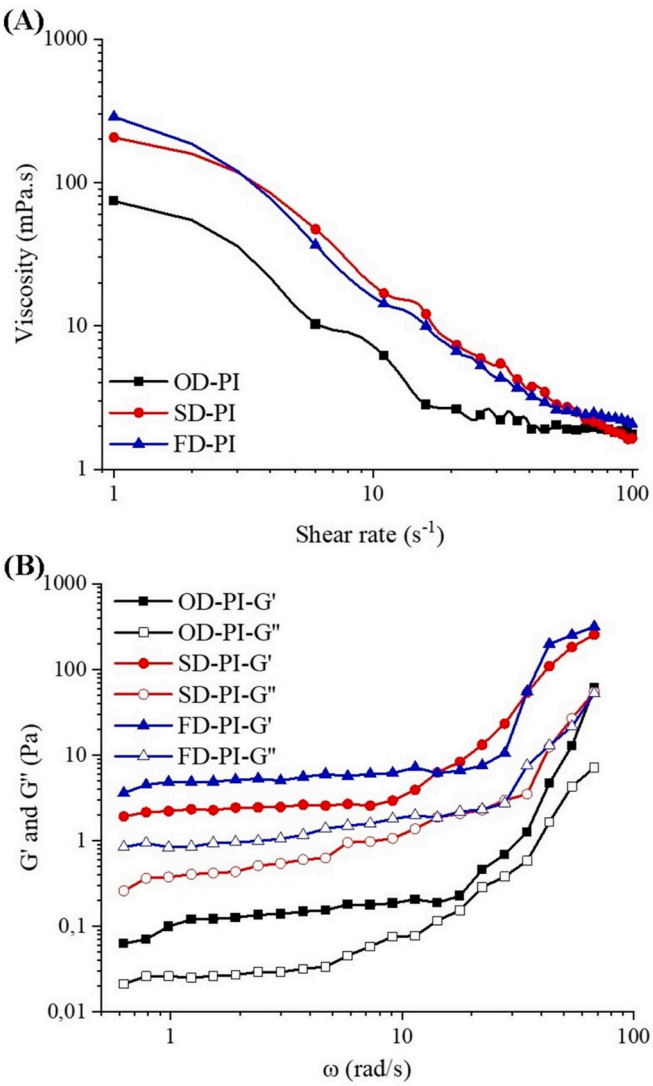

Fig. 4. Steady (a) and dynamic (b) rheological properties of the sesame protein isolates dried with different drying techniques (OD-PI: hot air dried sesame protein isolate; SD-PI: spray dried sesame protein isolate; FD-PI: freeze-dried sesame protein isolate).

to the higher shear rate, which is significantly greater than the effects of random motion caused by the Brown effect (Dabbour et al., 2021). Consistent with the trend of emulsion capacity and stability, the SD-PI sample had a relatively higher viscosity than the FD-PI samples, and the OD-PI samples had the lowest viscosity at a shear rate of 50 1/s, which is an accepted representative shear rate for swallowing. This phenomenon could be explained by lower particle size and higher protein solubility, resulting in more protein-water interactions (Baskinci and Gul, 2023), which is described in water-holding capacities (Table 2). In addition, the protein structural changes during SD are primarily to blame for the high viscosity achieved. These changes increase binding effectiveness (to H_2O molecules) by exposing the hidden hydrophobic/hydrophilic clusters and sites to the surrounding water (Dabbour et al., 2021).

Eq. (8) was used to evaluate the difference in power law constants, including consistency coefficient (K) and flow behavior index (n), which were impacted by drying techniques.

$$\tau = K \times \dot{\gamma}^n \quad (8)$$

where τ refers to the shear stress (Pa), K refers to the consistency index

(Pa.s^n), $\dot{\gamma}$ refers to the shear rate (1/s), and n refers to the flow behavior index (dimensionless).

The Oswald de Waele model fits all flow curves, which exhibit non-Newtonian shear-thinning behavior with a high determination coefficient ($R^2 > 0.955$; Table 4), indicating that the current model correctly represents the rheological characteristics of all sesame protein isolate solutions. The n values of the proteins were determined in a range from 0.029 to 0.091, which is below 1, implying that all samples exhibited shear-thinning flow characteristics, and the fluid nature was not changed. Moreover, the n values of solutions were in order OD-PI>FD-PI>SD-PI, indicating that drying methods significantly affected the flowing behavior of sesame protein isolate. The highest K value was recorded for SD-PI, followed by FD-PI and OD-PI, verifying the viscosity order for the corresponding protein solutions.

Oscillatory shear application is a key parameter because it gives an opinion on understanding the effect of protein interactions on the network structure of the protein macromolecules. Dynamic mechanical characterization to determine the viscoelastic or viscous properties of sesame seed protein concentrate samples was also performed, and storage modulus (G′) and loss modulus (G″), as the leading indicators of dynamic rheological characteristics that describe the viscosity and elasticity of suspensions, are given in Fig. 4b. All protein samples dried using different techniques showed solid gel-like behavior due to a higher storage modulus (G′) than loss modulus (G″). A similar result was reported by Wang, Niu, et al. (2022) for *Clanis bilineata tingtauica Mell* protein dried by different techniques. During the frequency increase until approximately 10 rad/s, G′ remained relatively constant, revealing that no further polymer ordering or reordering occurred within the network. For all samples, an increase in frequency caused an increase in both G′ and G″ values after 10 rad/s. The great frequency dependence of G′ and G″ values suggests no specific interaction between molecules (Joshi et al., 2011). It was also observed that the SD-PI exhibited much higher G′ and G″ than those of both OD-PI and FD-PI samples, which indicated a stronger gel structure. The better dynamical rheological properties could be explained by smaller particle size, higher solubility and H_0, and more free –SH group of SD-PI. The gel network structure was stable throughout the testing period, as evidenced by the G′ and G″ values for all protein samples remaining constant over time during the time sweep experiments (Joshi et al., 2011).

Since the G′ and G″ values of sesame protein suspensions tended to increase as the oscillation frequency increased, these moduli could be modeled as a power function of oscillatory frequency (Eqs. 9 and 10).

$$G' = K'(\omega)^{n'} \quad (9)$$

$$G'' = K''(\omega)^{n''} \quad (10)$$

where K′ and K″ refer to Power-law modulus constants (Pa.s), n’ and n” refer to the frequency exponents, ω and ω refers to the angular frequency (rad/s).

As shown in Table 4, high values of R^2 (>0.900) indicate that the moduli of suspensions fitted to the power law equation. All the K′ values were higher than K″, suggesting a viscoelastic structure (Gul et al., 2023). The highest K′ and K″ values were determined for SD-PI samples, indicating a more solid-like viscoelastic character. The n’′ values were higher than n’, indicating that G″ was more dependent on angular frequency.

3.8. *In vitro digestibility*

In vitro protein digestibility, an index to evaluate a food protein’s nutritional quality, indicates the amount of protein hydrolyzed by the digestive enzymes and absorbed by the organism. Better hydrolysis of proteins by enzymes (pepsin, trypsin, pancreatin) increases digestibility and means higher nutritional value. Fig. 5 displays the in vitro digestibility of the sesame protein isolate samples after INFOGEST static in vitro digestion. Since the residence period was brief and oral amylase is known to have little effect on protein digestion, the digesta was not examined following the simulated oral phase (Guo et al., 2021). As shown, in vitro digestibility was higher in the simulated intestinal phase than in the simulated gastric phase in all samples. A similar result was also found by (Colosimo, Warren, Finnigan, & Wilde, 2020), who stated that there was a significant increase in protein release after the transition from the simulated gastric phase to the simulated small intestine phase. Protein release was detected in the range of 34.24–39.89 % and 70.69–80.02 % in the simulated gastric and intestinal phases, respectively and the highest protein release in both phases was detected in the SD-PI sample, followed by FD-PI-PI and OD samples. While no significant difference was detected between the samples in terms of protein release in the simulated gastric phase ($P > 0.05$), the difference between the samples in the simulated intestinal phase was statistically significant ($P < 0.05$). The differences in protein release could be due to different particle sizes, water solubility, and denaturation of the protein. The

Table 4
Rheological properties of sesame seed protein isolates fabricated by different drying methods.

Samples	$\eta_{app} = K \times \dot{\gamma}^{n-1}$					
	K (Pa.s^n)	n (–)		R^2	η_{50} (mPa.s)	
OD-PI	0.11 ± 0.002^c	0.139 ± 0.005^a		0.955	2.037 ± 0.18^c	
SD-PI	0.43 ± 0.061^a	0.056 ± 0.002^c		0.941	2.949 ± 0.35^a	
FD-PI	0.31 ± 0.052^b	0.091 ± 0.023^b		0.969	2.691 ± 0.27^b	
	$G' = K'(\omega)^{n'}$			$G'' = K''(\omega)^{n''}$		
	K' (Pa)	n'	R^2	$K'' \times 10^{-5}$ (Pa)	n''	R^2
OD-PI	0.002 ± 0.001^c	2.438 ± 0.041^a	0.939	2.161 ± 0.118^c	3.421 ± 0.161^a	0.990
SD-PI	0.056 ± 0.004^a	2.070 ± 0.022^c	0.941	4.896 ± 0.094^a	3.289 ± 0.089^a	0.985
FD-PI	0.025 ± 0.003^b	2.203 ± 0.018^b	0.989	4.128 ± 0.077^b	3.344 ± 0.054^a	0.994

OD-PI: hot air dried sesame protein isolate; SD-PI: spray dried sesame protein isolate; FD-PI: freeze-dried sesame protein isolate. The superscript letters in the same column show statistical significance among the drying methods ($p < 0.05$).

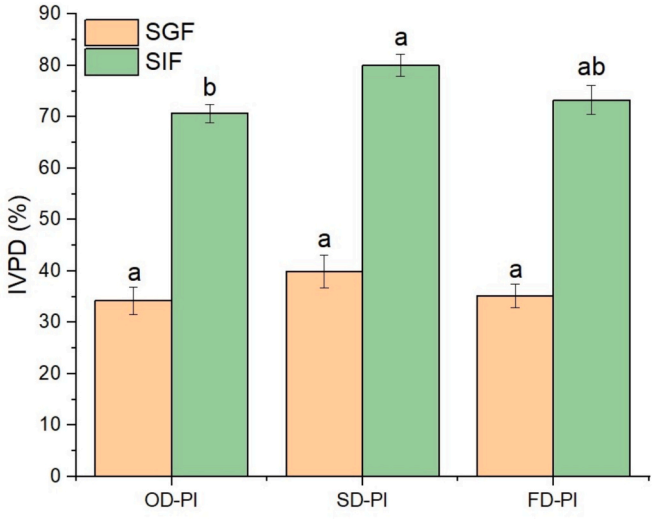

Fig. 5. In vitro digestibility of the sesame protein isolates dried with different drying techniques (OD-PI: hot air dried sesame protein isolate; SD-PI: spray dried sesame protein isolate; FD-PI: freeze-dried sesame protein isolate; SGF: simulated gastric fluid; SIF: simulated intestinal fluid).

small particle size increases the contact surface area, allowing the enzymes to access more particles, thus promoting rapid protein release. Also, increased water-protein interactions can lead to increased protein solubility, greater protein swelling, and a looser protein structure, making proteins more susceptible to hydrolysis by digestive enzymes. Moreover, a high unordered structure (random coil) contributes to high protein solubility. This phenomenon was consistent with particle size, FTIR (random coil), and water solubility measurements. Moreover, the hydrophobic groups are exposed by the denaturation of proteins, exposing hydrophobic residues to the surrounding, and protein digestibility benefits from this unfolding of tertiary and secondary structures, which is known as protein denaturation (Mathews et al., 2023; Nouska et al., 2024; Wang, Saxena, Vanga, & Raghavan, 2022). The binding site of the enzymes to the protein is the area of the hydrophobic group. Therefore, the presence of fewer hydrophobic groups and binding sites on the surface of OD-PI could explain the lower digestibility under gastrointestinal conditions compared to SD-PI and FD-PI (Table 2, H_0).

4. Conclusion

The present study provides a comprehensive evaluation of the structural, thermal, functional, rheological properties, and in vitro digestibility of sesame protein isolate (SPI) subjected to different drying techniques. While the proximate composition of the protein isolates remained unaffected by the drying methods, significant differences were observed in their physical, structural, and conformational attributes. These alterations, in turn, influenced the thermal behavior, techno-functional properties, and rheological performance of the proteins.

Among the techniques investigated, spray-dried SPI (SD-PI) demonstrated superior techno-functional and rheological properties, characterized by smaller particle size and higher solubility. Freeze-dried SPI (FD-PI), on the other hand, exhibited the highest levels of free sulfhydryl (–SH) groups and surface hydrophobicity, reflecting moderate structural unfolding and enhanced exposure of functional groups. Oven-dried SPI (OD-PI) displayed relatively higher thermal stability, which was consistent with its compact structure and crystallinity.

These observations were supported by FTIR and DSC analyses, which revealed distinct differences in secondary structure and thermal transitions across drying treatments. Furthermore, SD-PI exhibited significantly higher in vitro digestibility in simulated gastrointestinal fluids compared to FD-PI and OD-PI, likely due to its partially unfolded, more accessible structure.

Overall, the findings underscore that drying techniques exert a pronounced influence on the structural, functional, and nutritional properties of sesame protein isolates. Spray drying, in particular, emerges as a promising method for producing high-quality protein powders suitable for food applications where solubility, functionality, and digestibility are critical.

CRediT authorship contribution statement

Osman Gul: Writing – original draft, Methodology, Investigation. **Abdullah Akgün:** Writing – review & editing, Methodology, Investigation, Data curation. **Safa Karaman:** Writing – review & editing, Methodology, Investigation. **Mahmut Ekrem Parlak:** Writing – review & editing, Methodology, Investigation. **Furkan Turker Sarıcaoğlu:** Writing – review & editing, Validation, Methodology, Investigation, Data curation. **Senay Simsek:** Writing – review & editing, Supervision, Project administration, Methodology.

Declaration of competing interest

The authors declare that they have no known competing financial interests or personal relationships that could have appeared to influence the work reported in this paper.

Data availability

Data will be made available on request.

References

Achouri, A., Nail, V., & Boye, J. I. (2012). Sesame protein isolate: Fractionation, secondary structure and functional properties. *Food Research International, 46*(1), 360–369. https://doi.org/10.1016/j.foodres.2012.01.001

Aluko, R. E., & Monu, E. (2003). Functional and bioactive properties of quinoa seed protein hydrolysates. *Journal of Food Science, 68*(4), 1254–1258. https://doi.org/10.1111/j.1365-2621.2003.tb09635.x

AOAC. (2000). *Official methods of analysis* (17th ed.). Gaithersburg, Md: AOAC.

Arzeni, C., Martínez, K., Zema, P., Arias, A., Pérez, O. E., & Pilosof, A. M. R. (2012). Comparative study of high intensity ultrasound effects on food proteins functionality. *Journal of Food Engineering, 108*(3), 463–472. https://doi.org/10.1016/j.jfoodeng.2011.08.018

Barth, A. (2007). Infrared spectroscopy of proteins. *Biochimica et Biophysica Acta, 1767*(9), 1073–1101. https://doi.org/10.1016/j.bbabio.2007.06.004

Baskinci, T., & Gul, O. (2023). Modifications to structural, techno-functional and rheological properties of sesame protein isolate by high pressure homogenization. *International Journal of Biological Macromolecules, 250*, Article 126005. https://doi.org/10.1016/j.ijbiomac.2023.126005

Brishti, F. H., Chay, S. Y., Muhammad, K., Ismail-Fitry, M. R., Zarei, M., Karthikeyan, S., & Saari, N. (2020). Effects of drying techniques on the physicochemical, functional, thermal, structural and rheological properties of mung bean (Vigna radiata) protein isolate powder. *Food Research International, 138*(Pt B), Article 109783. https://doi.org/10.1016/j.foodres.2020.109783

Colosimo, R., Warren, F. J., Finnigan, T. J. A., & Wilde, P. J. (2020). Protein bioaccessibility from mycoprotein hyphal structure: In vitro investigation of underlying mechanisms. *Food Chemistry, 330*, Article 127252. https://doi.org/10.1016/j.foodchem.2020.127252

Dabbour, M., Sami, R., Mintah, B. K., He, R., Wahia, H., Khojah, E., … Fikry, M. (2021). Effect of drying techniques on the physical, functional, and rheological attributes of isolated sunflower protein and its hydrolysate. *Processes, 10*(1). https://doi.org/10.3390/pr10010013

De Maria, S., Ferrari, G., & Maresca, P. (2016). Effects of high hydrostatic pressure on the conformational structure and the functional properties of bovine serum albumin. *Innovative Food Science & Emerging Technologies, 33*, 67–75. https://doi.org/10.1016/j.ifset.2015.11.025

Deak, N. A., & Johnson, L. A. (2006). Functional properties of protein ingredients prepared from high-sucrose/low-stachyose soybeans. *Journal of the American Oil Chemists' Society, 83*, 811–818.

Dong, X., Woo, M. W., & Quek, S. Y. (2024). The physicochemical properties, functionality, and digestibility of hempseed protein isolate as impacted by spray drying and freeze drying. *Food Chemistry, 433*, Article 137310. https://doi.org/10.1016/j.foodchem.2023.137310

Ellman, G. L. (1959). Tissue sulfhydryl groups. *Archives of Biochemistry and Biophysics, 82*(1), 70–77.

Embaby, H. E. S. (2010). Effect of heat treatments on certain antinutrients and in vitro protein digestibility of peanut and sesame seeds. *Food Science and Technology Research, 17*(1), 31–38.

Feyzi, S., Varidi, M., Zare, F., & Varidi, M. J. (2018). Effect of drying methods on the structure, thermo and functional properties of fenugreek (Trigonella foenum graecum) protein isolate. *Journal of the Science of Food and Agriculture, 98*(5), 1880–1888. https://doi.org/10.1002/jsfa.8669

Ghribi, A. M., Gafsi, I. M., Blecker, C., Danthine, S., Attia, H., & Besbes, S. (2015). Effect of drying methods on physico-chemical and functional properties of chickpea protein concentrates. *Journal of Food Engineering, 165*, 179–188. https://doi.org/10.1016/j.jfoodeng.2015.06.021

Gong, K.-J., Shi, A.-M., Liu, H.-Z., Liu, L., Hu, H., Adhikari, B., & Wang, Q. (2016). Emulsifying properties and structure changes of spray and freeze-dried peanut protein isolate. *Journal of Food Engineering, 170*, 33–40. https://doi.org/10.1016/j.jfoodeng.2015.09.011

Gul, O., Saricaoglu, F. T., Atalar, I., Gul, L. B., Tornuk, F., & Simsek, S. (2023). Structural characterization, Technofunctional and rheological properties of sesame proteins treated by high-intensity ultrasound. *Foods, 12*(9). https://doi.org/10.3390/foods12091791

Guo, Q., Bayram, I., Zhang, W., Su, J., Shu, X., Yuan, F., … Gao, Y. (2021). Fabrication and characterization of curcumin-loaded pea protein isolate-surfactant complexes at neutral pH. *Food Hydrocolloids, 111*. https://doi.org/10.1016/j.foodhyd.2020.106214

Hahm, T.-S., & Kuei, C.-Y. (2015). Present and potential industrial applications of sesame: A Mini review. *Journal of Food Processing and Preservation, 39*(6), 3137–3144. https://doi.org/10.1111/jfpp.12381

Hu, H., Wu, J., Li-Chan, E. C. Y., Zhu, L., Zhang, F., Xu, X., … Pan, S. (2013). Effects of ultrasound on structural and physical properties of soy protein isolate (SPI) dispersions. *Food Hydrocolloids, 30*(2), 647–655. https://doi.org/10.1016/j.foodhyd.2012.08.001

Hu, X.-Z., Cheng, Y.-Q., Fan, J.-F., Lu, Z.-H., Yamaki, K., & Li, L.-T. (2010). Effects of drying method on physicochemical and functional properties of soy protein isolates. *Journal of Food Processing and Preservation, 34*(3), 520–540. https://doi.org/10.1111/j.1745-4549.2008.00357.x

Joshi, M., Adhikari, B., Aldred, P., Panozzo, J. F., & Kasapis, S. (2011). Physicochemical and functional properties of lentil protein isolates prepared by different drying methods. *Food Chemistry, 129*(4), 1513–1522. https://doi.org/10.1016/j.foodchem.2011.05.131

Klompong, V., Benjakul, S., Kantachote, D., & Shahidi, F. (2007). Antioxidative activity and functional properties of protein hydrolysate of yellow stripe trevally (Selaroides leptolepis) as influenced by the degree of hydrolysis and enzyme type. *Food Chemistry, 102*(4), 1317–1327. https://doi.org/10.1016/j.foodchem.2006.07.016

Laemmli, U. K. (1970). SDS-page Laemmli method. *Nature, 227*, 680–685.

Li, N., Wang, Y., Gan, Y., Wang, S., Wang, Z., Zhang, C., & Wang, Z. (2022). Physicochemical and functional properties of protein isolate recovered from Rana chensinensis ovum based on different drying techniques. *Food Chemistry, 396*, Article 133632. https://doi.org/10.1016/j.foodchem.2022.133632

Lin, N., Liu, B., Liu, Z., & Qi, T. (2020). Effects of different drying methods on the structures and functional properties of phosphorylated Antarctic krill protein. *Journal of Food Science, 85*(11), 3690–3699. https://doi.org/10.1111/1750-3841.15503

Mathews, A., Tangirala, A. D. S., Thirunavookarasu, S. N., Kumar, S., Anandharaj, A., & Rawson, A. (2023). Extraction and modification of protein from sesame oil cake by the application of emerging technologies. *Food Chemistry Advances, 2*. https://doi.org/10.1016/j.focha.2023.100326

Minekus, M., Alminger, M., Alvito, P., Ballance, S., Bohn, T., Bourlieu, C., … Brodkorb, A. (2014). A standardised static in vitro digestion method suitable for food - an international consensus. *Food & Function, 5*(6), 1113–1124. https://doi.org/10.1039/c3fo60702j

Mune, M. A. M., & Sogi, D. S. (2015). Emulsifying and foaming properties of protein concentrates prepared from cowpea and Bambara bean using different drying methods. *International Journal of Food Properties, 19*(2), 371–384. https://doi.org/10.1080/10942912.2015.1023399

Mune Mune, M. A., Sogi, D. S., & Minka, S. R. (2017). Response surface methodology for investigating structure–function relationship of grain legume proteins. *Journal of Food Processing and Preservation, 42*(2). https://doi.org/10.1111/jfpp.13524

Nan, J., Zou, M., Wang, H., Xu, C., Zhang, J., Wei, B., … Xu, Y. (2018). Effect of ultra-high pressure on molecular structure and properties of bullfrog skin collagen. *International Journal of Biological Macromolecules, 111*, 200–207. https://doi.org/10.1016/j.ijbiomac.2017.12.163

Nie, H. N., Dong, H., Chen, Y. L., Hao, M. M., Chen, J. N., Tang, Z. C., … Xue, Y. L. (2023). Effects of spray drying and freeze drying on the structure and emulsifying properties of yam soluble protein: A study by experiment and molecular dynamics simulation. *Food Chemistry, 409*, Article 135238. https://doi.org/10.1016/j.foodchem.2022.135238

Nikoo, M., Benjakul, S., & Xu, X. (2015). Antioxidant and cryoprotective effects of Amur sturgeon skin gelatin hydrolysate in unwashed fish mince. *Food Chemistry, 181*, 295–303. https://doi.org/10.1016/j.foodchem.2015.02.095

Nouska, C., Deligeorgaki, M., Kyrkou, C., Michaelidou, A.-M., Moschakis, T., Biliaderis, C. G., & Lazaridou, A. (2024). Structural and physicochemical properties of sesame cake protein isolates obtained by different extraction methods. *Food Hydrocolloids, 151*. https://doi.org/10.1016/j.foodhyd.2024.109757

Özdemir, E. E., Görgüç, A., Gençdağ, E., & Yılmaz, F. M. (2022). Physicochemical, functional and emulsifying properties of plant protein powder from industrial sesame processing waste as affected by spray and freeze drying. *Lwt, 154*. https://doi.org/10.1016/j.lwt.2021.112646

Petruccelli, S., & Añón, M. C. (1996). pH-induced modifications in the thermal stability of soybean protein isolates. *Journal of Agricultural and Food Chemistry, 44*(10), 3005–3009.

dos Santos, S. D. A., Martins, V. G., Salas-Mellado, M., & Prentice, C. (2011). Evaluation of functional properties in protein hydrolysates from bluewing Searobin (Prionotus punctatus) obtained with different microbial enzymes. *Food and Bioprocess Technology, 4*(8), 1399–1406. https://doi.org/10.1007/s11947-009-0301-0

Shen, Y., Tang, X., & Li, Y. (2021). Drying methods affect physicochemical and functional properties of quinoa protein isolate. *Food Chemistry, 339*, Article 127823. https://doi.org/10.1016/j.foodchem.2020.127823

Tang, C.-H., & Jiang, Y. (2007). Modulation of mechanical and surface hydrophobic properties of food protein films by transglutaminase treatment. *Food Research International, 40*(4), 504–509. https://doi.org/10.1016/j.foodres.2006.09.010

Wang, J., Saxena, R., Vanga, S. K., & Raghavan, V. (2022). Effects of microwaves, ultrasonication, and Thermosonication on the secondary structure and digestibility of bovine Milk protein. *Foods, 11*(2). https://doi.org/10.3390/foods11020138

Wang, S., Niu, L., Zhou, B., Peng, Y., Yang, X., Shen, Y., & Li, S. (2022). Drying methods affect physicochemical and functional characteristics of Clanis Bilineata Tingtauica mell protein. *Frontiers in Nutrition, 9*, Article 1053422. https://doi.org/10.3389/fnut.2022.1053422

Waterborg, J. H. (2009). The Lowry method for protein quantitation. *The Protein Protocols Handbook*, 7–10.

Wei, P., Zhao, F., Wang, Z., Wang, Q., Chai, X., Hou, G., & Meng, Q. (2022). Sesame (*Sesamum indicum L.*): A comprehensive review of nutritional value, phytochemical composition, health benefits, development of food, and industrial applications. *Nutrients, 14*(19). https://doi.org/10.3390/nu14194079

Ye, M., Wang, Z., Yan, X., Zeng, Z., Peng, T., Xia, J., … Yu, P. (2024). Effects of drying methods on the physicochemical and functional properties of Cinnamomum camphora seed kernel protein isolate. *Foods, 13*(6). https://doi.org/10.3390/foods13060968

Zhang, M., Wang, O., Cai, S., Zhao, L., & Zhao, L. (2023). Composition, functional properties, health benefits and applications of oilseed proteins: A systematic review. *Food Research International, 171*, Article 113061. https://doi.org/10.1016/j.foodres.2023.113061

Zhao, Q., Wang, L., Hong, X., Liu, Y., & Li, J. (2021). Structural and functional properties of perilla protein isolate extracted from oilseed residues and its utilization in Pickering emulsions. *Food Hydrocolloids, 113*. https://doi.org/10.1016/j.foodhyd.2020.106412

Zhao, Q., Xiong, H., Selomulya, C., Chen, X. D., Huang, S., Ruan, X., … Sun, W. (2013). Effects of apray drying and freeze drying on the properties of protein isolate from rice dreg protein. *Food and Bioprocess Technology, 6*(7), 1759–1769. https://doi.org/10.1007/s11947-012-0844-3